Gold and silver oxide conducting nanocomposite cathode for glucose biofuel cell

Saikat Banerjee, Mathew Nguyen, and Gymama Slaughter (IEEE Senior Member)
Center for Bioelectronics, Department of Electrical and Computer Engineering, Old Dominion University, Norfolk, VA-23528, USA.

***Abstract*—A glucose biofuel cell on a flexible bacterial nanocellulose film was prepared. The bioelectrodes were printed using gold ink as the conductive material. The anode was modified with colloidal platinum for the oxidation of glucose. The cathode was modified with a nanocomposite comprising gold nanoparticles (AuNPs) and silver oxide (Ag_2O) nanoparticles. The cathode was characterized via cyclic voltammetry (CV), electrochemical impedance spectroscopy (EIS), and UV spectroscopy techniques. The assembled biofuel cell generated a maximum open circuit voltage (V_{oc}) of 0.485 V, short circuit current (I_{sc}) of 0.352 mA/cm^2, and a maximum peak power density (P_{max}) of 0.032 mW/cm^2 when operating in 30 mM concentration. This system showed a stable and linear performance with a linear range of 1 mM to 30 mM glucose. The gold printed electrode process is applicable to the development of wearable and implantable abiotic biofuel cell.**

Keywords—abiotic, gold nanoparticles, silver oxide nanoparticles

I. Introduction

Nanostructures continue to gain significant attention because of their broad application in the development of new diagnostic and therapeutic tools [1-3]. They have been employed in the development of drug delivery and antimicrobial systems, cell-based assays, and analytical tools such as sensors and fuel cells [4]. Gold nanoparticles (AuNPs) are promising nanomaterial for use in catalysis, water purification, and contamination detection [5, 6]. Their electronic configuration and oxidation resistance make them unique among other metallic nanoparticles for the construction of biofuel cells. Glassy carbon-based biofuel cell system with gold nanoparticles and laccase as anodic and cathodic electrodes, respectively have been demonstrated to generate adequate power density [7]. Zeng et al., employed nickel oxide nanoparticles with graphene nanosheet as the anodic electrode in the fabrication of non-enzymatic glucose biofuel cell [8]. The biofuel cell operating on 0.1M KOH containing 0.1M glucose produced a 0.7 V. Although biofuel cells are seen as an alternative power sources for wearable and implantable devices that can be used in remote areas, additional research and development are required for the improvement of the current and power densities produced by biofuel cells and to design a cell that enables long-term stable operation.

In this work, gold electrodes were printed onto flexible bacterial nanocellulose film. The anode was modified with electrodeposited colloidal platinum (co-Pt) for the oxidation of glucose. The surface of the cathode was modified with gold nanoparticles (AuNPs) and silver oxide (Ag_2O) nanoparticles to create a nanocomposite that promotes the reduction of dissolved oxygen to water. Electrochemical techniques, UV spectroscopy, and impedance spectroscopy were carried out to characterize the modified cathode. The biofuel cell demonstrated stable operations and a wide linear dynamic range of 1 to 30 mM glucose.

The research presented in this article was supported by the National Science Foundation Award #1921364 and #1925806.

II. Experimental section

A. Materials

Silver nitrate, chloroauric acid, polyethylene glycol 3000 (PEG), sodium hydroxide, D (+) glucose, potassium phosphate monobasic, sodium azide, and Nafion were obtained from Sigma-Aldrich. The platinizing solution was purchased from YSI Inc., and NGP-J gold nanoparticle ink was acquired from Iwatani Corporation of America. The multiwalled carbon nanotube NINK-1000 was obtained from Nanolab, Inc. All the solutions were prepared with 18.2 MΩ-cm Milli-Q water. Platinum counter electrode, Ag/AgCl reference electrode, and PalmSense4 potentiostat were purchased from BASI Inc. Electrode Fabrication

Synthesis of AuNPs. AuNPs were synthesized using previously established protocols [4]. Briefly, 2.8 mL of gold (III) chloride trihydrate solution, which was added to 80 mL of ultrapure water and stirred in an ice bath. A 1.0 mL of 0.01M $Na_3C_6H_5O_7$ was added to reaction mixture and stirred in an ice bath for 30 minutes. In the interim, 0.1M $NaBH_4$ solution was prepared and cooled in an ice bath separately. Afterward, 1.5 mL of $NaBH_4$ was injected into the gold solution and stirred. Rapid reduction of gold (III) was observed via a color change of yellow to wine red. The solution was stored at 4 °C overnight when not in use.

Synthesis of Ag_2O. Silver oxide nanoparticles (Ag_2O) solution was prepared by dissolving 20 g of PEG in 1 L of reverse osmosis water, which was then heated to 75 ºC under constant stirring for 1 h to ensure that all the PEG was completely dissolved to form a homogeneous solution. The resulting PEG solution was filtered using Whatman ashless filter papers to remove any impurities. Under constant stirring, silver nitrate solution was prepared from 0.5 g of silver nitrate and was added to the prepared PEG solution at 75 ºC for 1 h. The pH was maintained at pH 9.8 to 10 throughout the reaction process using 0.1 M NaOH solution. Subsequently, the Ag_2O particles precipitated to the bottom of the solution and the solution was centrifuged to extract the particles from the original solution.
Preparation of anode and cathode. Colloidal platinum (co-Pt) was electrodeposited on gold printed nanocellulose electrode

(*thickness* = 130 µm) using a three-electrode configuration consisting of the anodic working electrode, platinum counter electrode, and Ag/AgCl reference electrode immersed in platinizing solution. The co-Pt was electrodeposited onto the surface on the printed gold electrode at an applied potential of −225 mV vs. Ag/AgCl for 1500 s. The electrode was then washed with DI water and dried a 80 ºC for 30 minutes, followed by cooling in ambient air. For the cathode, 20 µL of AuNPs solution was mixed in with the Ag_2O solution using ultra-sonication for 30 minutes to form the AuNPs-Ag_2O solution. The AuNPs-Ag_2O solution was drop casted onto gold printed bacterial nanocellulose electrode surface, followed by soft baking at 60 ºC for 30 minutes. For easy handling and device testing, a tungsten wire was attached to the electrodes using carbon wire glue.

B. Electrical Measurements

Electrochemical measurements were performed using Palmsense4 electrochemical workstation. The electrochemical cell consist of a conventional three electrode system where the co-Pt or AuNP-Ag_2O-MWCNTs was used as a working electrode, Ag/AgCl (3 M KCl) as the reference electrode and a platinum wire as the counter electrode for characterizing the anode and cathode electrodes, respectively. All electrochemical experiments were carried out at room temperature (25.0 ± 0.5 ◦C) in an electrochemical cell.

III. Results & Discussion

A. UV- Vis Absorption Spectrum Analysis

UV-Vis spectroscopy was performed to confirm the synthesis of AuNPs and Ag_2O nanoparticles. Figure 1A shows an absorbance peak at 240 nm with a broad tail in the visible region. This indicates the presence of spherical Ag_2O nanoparticles and is correlated with the resonant excitations of the surface plasmon and interband transitions [9, 10]. A broad band in the range 504 nm to 540 nm was observed for the AuNPs and two smaller but prominent peaks at 405 nm and 690 nm show different size of AuNPs (Figure 1B). The peak at 530 nm indicates spherical nanoparticles in the size range of 3 nm to 60 nm [11, 12]. The optical absorption at ca. 300 - 600 nm shows the clustering of gold nanoparticles [13]. The peak shift towards the longer wavelength is attrributed to the dephasing of signals from individual plasmons due to increased size and dispersion of the AuNPs [14]. Therefore, the different sizes of AuNPs in solution resulted in the generation of multiple peaks [15]. The resultant peaks at 340 nm and 600 nm were observed for the combined Ag_2O and AuNPs as shoewn in Figure 1C. The red shifting and broadening of the peaks may be due to the attachment of the two particles to generate an absorption spectrum common to that of a single rod-like particle [16] or the nanoparicles forming small metallic clusters [17].

B. Cyclic Voltammetry

The cyclic voltammogram in Figure 2 shows the catalytic behavior of the cathode in air and oxygen saturated conditions. The electrode was placed in non-stirring PBS in air and under oxygen purging for 5 and 10 minutes to achieve oxygen saturation conditions. The shape of the voltammogram is

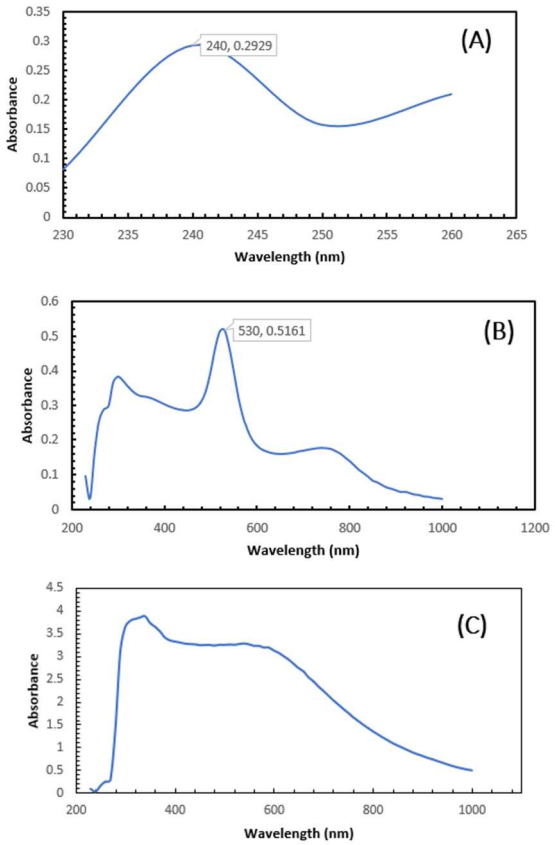

Fig. 1. A schematic diagram of the bioelectrode design and photomicrograph of LIG on the plastic platform.

consistent with those previously reported [18]. From the voltammogram, it is apparent that the reduction current density increases in the presence of oxygen with an onset potential of 0.231 V in a similar manner to oxygen reduction at noble metal or enzyme-based cathodes [4]. The reduction peak observed is due to the presence of silver, which results in a reduction reaction that is independent of the electrolyte environment. The

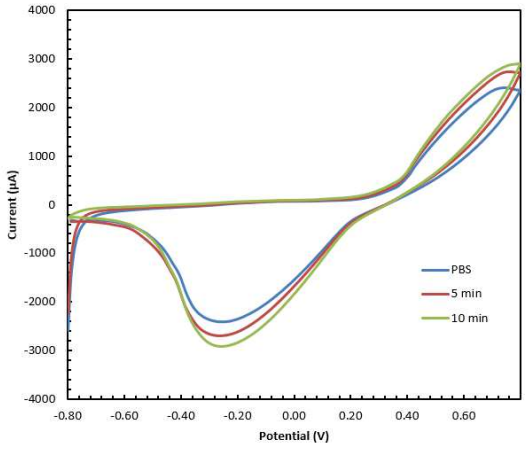

Fig. 2. Cyclic voltammogram of AuNPs-Ag_2O cathode in PBS with O_2 saturated PBS for 5 min and 10 min in 0.1 M PBS pH 7.4 and 50 mV/s against Ag /AgCl.

incorporation of AuNPs into the cathode material impacts the electrocatalytic behavior observed and can also be attributed to the decreased porosity and lower reduction currents observed for the reduction of oxygen to water. The co-Pt glucose oxidation anode and the AuNPs-Ag_2O oxygen reduction cathode were used to evaluate the biofuel cell performance. The oxidation reaction at the anode produces electrons that travels through the external circuitry and recombines at the cathode for the reduction of oxygen to generate water and a stable current.

C. Impedance spectroscopy

The modified surface of the electrodes was characterized by EIS to analyze the electronic transmission properties of nanocomposites at the electrode-electrolyte interface. Figure 3A shows the Nyquist plot of the co-Pt anode exposed to increasing concentration of glucose. It can be observed that the electrical impedance decreases with the increase in glucose concentration. This can be attributed to the oxidation of glucose at the co-Pt electrode electrolyte interface. The EIS of Ag_2O-MWCNTs electrode and AuNPs-Ag2O-MWCNTs shows an increase in the phase angle and higher impedance were observed in 5 mM of potassium ferricyanide.

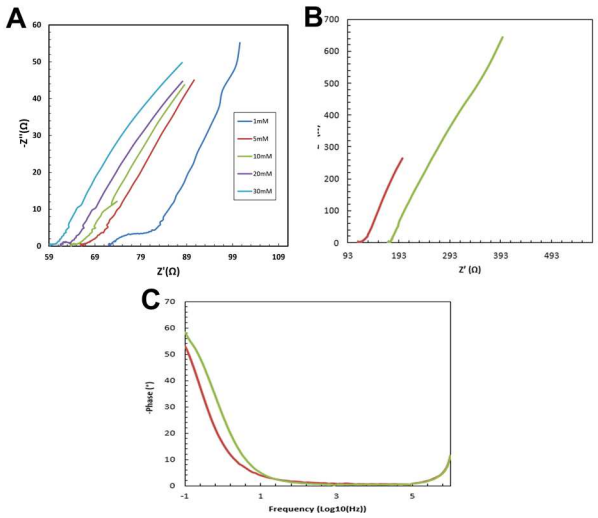

Fig. 3. (A) Nyquist plot of co-Pt anode in the presence of increasing concentration of glucose, (B) Ag_2O cathode (red) and AuNPs-Ag_2O (green), and (C) Bode plot of Ag_2O cathode (red) and AuNPs-Ag_2O (green) in 5mM $K(Fe_3(CN)_6)^3$.

D. Biofuel cell Characterization

Linear sweep voltammetry was conducted at 1 mV/s to generate the polarization and power curves of the glucose biofuel cell shown in Figures 4A and 4B, respectively. The open circuit voltage produced by the glucose biofuel cell in the presence of 30 mM glucose was 0.485 V. A short circuit current of 0.350 mA/cm² and a peak power density of 0.032 mW/cm² was observed in the presence of 30 mM glucose. The corresponding calibration curve shown in Figure 4C demonstrates that the peak power generated by the biofuel cell is directly proportional to the glucose concentration. A linear range of 1 mM to 30 mM (r^2 = 0.9680) with a sensitivity of 0.778 µW/mM-cm².

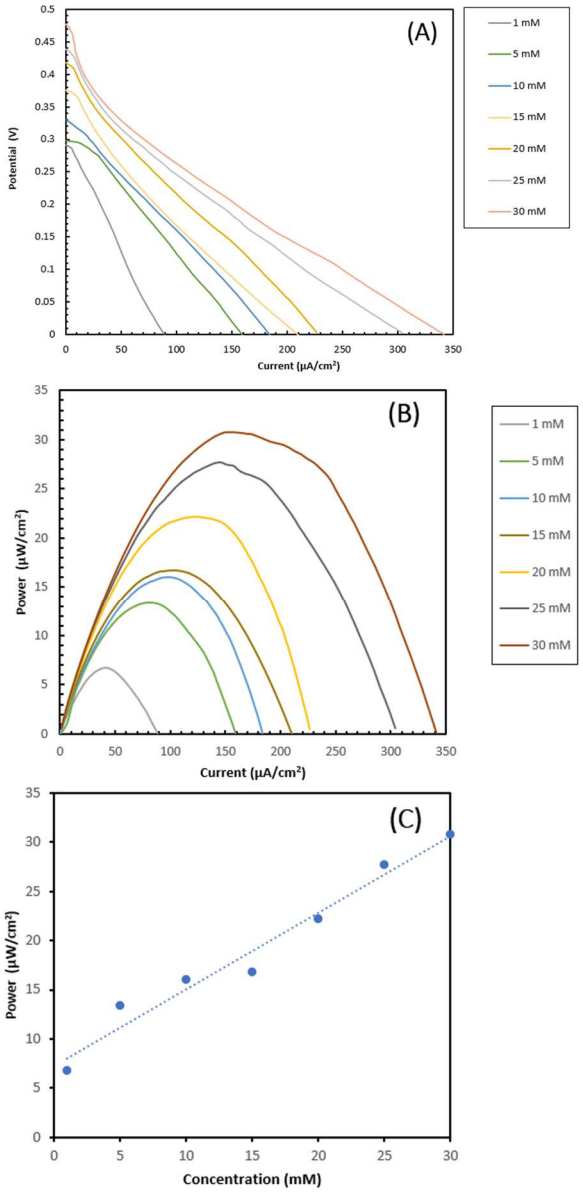

Fig. 4. (A) Polarization and (B) power curves in the presence of 1 mM to 30 mM glucose, and (C) corresponding calibration curve of peak power versus concentration.

IV. Conclusion

A biofuel cell employing AuNPs-Ag_2O-MWCNTs cathode was demonstrated to be capable of harnessing the biochemical energy of glucose when paired with co-Pt anode. UV spectroscopy revealed the individual peak and combinational characteristics of the nanoparticles used. The biofuel cell exhibited a linear range of 1 mM to 30 mM glucose and an open circuit voltage of 0.485 V and short circuit current of 0.352 mA/cm² with a maximum power of 0.032 mW/cm² in 30 mM glucose. The biofuel cell can serve as an alternative glucose biosensor requiring minimal circuit components and no external power supply.

REFERENCES

[1] T. Liyanage, A. Qamar, & G. Slaughter, "Nanomaterials for biosensors: A Review" IEEE Sensors Journal. vol. 21 (11), 12407-12425, 2021.

[2] G. Slaughter, "Fabrication of nanoindented electrodes for glucose detection." Journal of diabetes science and technology vol. 4(2), pp. 320-327, 2010.

[3] T. Liyanage, M. Lai, G. Slaughter. "Label-free tapered optical fiber plasmonic biosensor." Analytica Chimica Acta, 338629, 2021.

[4] J.S. Narayanan, & G. Slaughter. "Towards a dual in-line electrochemical biosensor for the determination of glucose and hydrogen peroxide." Bioelectrochemistry 128 pp. 56-65, 2019.

[5] A. Rinaldi, B. Mecheri, V. Garavaglia, S. Licoccia, P. Di Nardo, & E. Traversa, "Engineering materials and biology to boost performance of microbial fuel cells: a critical review," Energy & Environmental Science, vol 1(4), pp. 417-429, August 2008.

[6] B.E. Logan, B. Hamelers, R. Rozendal, U. Schröder, J. Keller, S. Freguia, P. Aelterman, W. Verstraete, & Rabaey, K, "Microbial fuel cells: methodology and technology," Environmental science & technology, vol 40(17), pp. 5181-5192, September 2006.

[7] F. Qu, X. Ma, Y. Hui, F. Chen, Y. Gao. "Preparation of Close - Packed Silver Nanoparticles on Graphene to Improve the Enzyme Immobilization and Electron Transfer at Electrode in Glucose/O2 Biofuel Cell." Chinese Journal of Chemistry, vol 35(7), pp.1098-1108, July 2017.

[8] G. Zeng, W. Li, S. Ci, J. Jia, Z. Wen. "Highly dispersed NiO nanoparticles decorating graphene nanosheets for non-enzymatic glucose sensor and biofuel cell." Scientific reports,vol 6(1), pp.1-8, November 2016.

[9] J.K. Jang, I.S. Chang, & B.H. Kim, " Improvement of cathode reaction of a mediatorless microbial fuel cell. Journal of Microbiology and Biotechnology," vol 14(2), pp. 324-329, 2004.

[10] F. Mafuné, J.Y. Kohno, Y. Takeda, T. Kondow, & H. Sawabe, "Structure and stability of silver nanoparticles in aqueous solution produced by laser ablation," The Journal of Physical Chemistry B, vol 104(35), pp. 8333-8337, August 2000.

[11] N.V. Tarasenko, A.V. Butsen, E.A. Nevar, & N.A. Savastenko, "Synthesis of nanosized particles during laser ablation of gold in water," Applied surface science, vol 252(13), pp. 4439-4444, April 2006.

[12] J.P. Sylvestre, A.V. Kabashin, E. Sacher, & M. Meunier, "Femtosecond laser ablation of gold in water: influence of the laser-produced plasma on the nanoparticle size distribution," Applied Physics A, vol 80(4), pp. 753-758, Februrary 2005.

[13] P.V. Kazakevich, A.V. Simakin, V.V. Voronov, & G.A. Shafeev, "Laser induced synthesis of nanoparticles in liquids," Applied Surface Science, vol 252(13), pp. 4373-4380, April 2006.

[14] F. Mafuné, J.Y. Kohno, Y. Takeda, & T. Kondow, "Full physical preparation of size-selected gold nanoparticles in solution: laser ablation and laser-induced size control," The Journal of Physical Chemistry B, vol 106(31), pp. 7575-7577. August 2002.

[15] A.V. Kabashin & M. Meunier, "Synthesis of colloidal nanoparticles during femtosecond laser ablation of gold in water," Journal of Applied Physics, vol 94(12), pp. 7941-7943, December 2003.

[16] A.V. Simakin, V.V. Voronov, G.A. Shafeev, R. Brayner, & F. Bozon-Verduraz, "Nanodisks of Au and Ag produced by laser ablation in liquid environment," Chemical Physics Letters, vol 348(3-4), pp. 182-186, November 2001.

[17] C.E. Rayford, G. Schatz, & K. Shuford, " Optical properties of gold nanospheres." Nanoscape, vol 2(1), pp. 27-33, 2005

[18] S. Banerjee, & G. Slaughter, "A tattoo-like glucose abiotic biofuel cell." J. Electroanalytical Chemistry, 2021.